1972

Optical Timing of the Crab Pulsar, NP 0532*

Paul E. Boynton

E. J. Groth III

D. P. Hutchinson

Bruce Partridge
Haverford College, bpartrid@haverford.edu

1972

Optical Timing of the Crab Pulsar, NP 0532*

P. E. Boynton

E. J. Groth III

D. P. Hutchinson

R. Bruce Partridge
Haverford College

THE ASTROPHYSICAL JOURNAL, 175:217–241, 1972 July 1

OPTICAL TIMING OF THE CRAB PULSAR, NP 0532*

P. E. BOYNTON,† E. J. GROTH, D. P. HUTCHINSON,‡ G. P. NANOS, JR.,
R. B. PARTRIDGE,§ AND D. T. WILKINSON‖
Joseph Henry Laboratories, Physics Department, Princeton
University, Princeton, New Jersey 08540
Received 1971 September 30; revised 1972 February 7

ABSTRACT

Absolute times of arrival of NP 0532 pulses have been measured over a 2-year period. The data are shown to be consistent with a cubic polynomial which describes the secular slowdown, a sudden increase and subsequent exponential decay of the frequency (the glitch of 1969 September 29), and an intrinsic $1/f$ noise component in the frequency.

I. INTRODUCTION

We have continued optical timing observations of the Crab pulsar, NP 0532. The preliminary results of these observations were described in Boynton *et al.* (1969*a*), where, on the basis of a data string only 40 days long, an anomalously large value for the braking index was reported. It now appears that the pulse frequency is undergoing a random walk (Groth 1971), which places a lower limit on the length of data required to find or measure a given effect. It was only after we recognized the existence of this noise component in the data that we were able to make progress in studying the other two important features in the data; the secular slowing down and the abrupt frequency jump of 1969 September 29.

In our interpretation of the data we have tried to employ the simplest and most plausible physical models which explain the time variations. For example, by including the noise component, we find it unnecessary to assume time-dependent braking, pulsar wobble, or planets around the pulsar. Two plausible physical processes—matter accretion and crustal cracking—are capable of producing the observed random walk in pulsar frequency.

II. APPARATUS

The instrumentation in use from 1969 August through the present is similar to that used in the spring of 1969. Several improvements were made, especially in the electronics, in order to improve the precision of the measurements. The frequency of the temperature-dependent CAT[1] sweep oscillator (refer to fig. 1 of Boynton *et al.* 1969*a*) is monitored so that the time per CAT channel is known for each run. The pulsar period is now derived from a 10-MHz oscillator, reducing the jitter in the starting time of CAT sweeps to 0.1 μs. Furthermore, the period of the trigger pulses generated by the 10-MHz oscillator is stable to better than 1 nanosecond and the unknown phase slippage is only 1.8 μs for our integration time of 2 minutes. With the substitution of a storage scope in place of

* This research was supported in part by the Office of Naval Research and the National Science Foundation.

† Present address: University of Washington, Seattle, Washington 98105.

‡ Present address: Stanford Linear Accelerator, Palo Alto, California 94305.

§ Present address: Haverford College, Haverford, Pennsylvania 19041.

‖ Alfred P. Sloan Fellow. On leave of absence at Institute for Astronomy, University of Hawaii, Honolulu, Hawaii 96822.

[1] Computer of average transients.

the CRT used to monitor Loran timing signals, the phase of our epoch pulse relative to Loran can usually be determined to 1 μs. However, there continue to be a few nights when Loran cycle identification is ambiguous and the relative phase of the epoch pulse and Loran may be in error by 10 μs. Thus, we continue to add 10 μs to the error estimates for all average arrival times. In many cases, this phase error is the dominant source of error and the assigned errors probably overestimate the true measurement errors.

In addition to the summertime gaps in the data when the pulsar is too near the Sun for optical observations, our data have gaps extending from 1970 February 7 to 1970 February 23, and from 1970 December 8 to 1971 January 17. The Loran-C 1-s pulse was off the air during the former interval, while in the latter the CAT was inadvertently adjusted to introduce an unknown delay into the measurements.

III. PULSE SHAPE

The location of the pulse in the CAT memory is found by least-squares fitting a master pulse shape to each run. This master pulse is derived by averaging over many runs, and is in agreement with other determinations of the pulse shape, notably that of Papaliolios, Carleton, and Horowitz (1970).

An important assumption, made throughout the analysis, is that the pulse shape is constant in time, at least when averaged over 3600 or more periods (the length of each integration). Were the pulse shape to vary, incorrect estimates for the arrival times would be obtained, although it is not clear how the phase of the pulse would be defined in such a case.

There are several ways to check the constancy of the pulse shape. One scheme is to study the distribution of minimum chi squares determined when the master shape is fitted to the individual runs. The χ^2 distribution for the 1969–1970 data is shown as the upper distribution in figure 1. Also shown is the distribution expected from counting statistics. The agreement between the two distributions indicates that any run-to-run variations in the pulse shape are smaller than the statistical uncertainties in measuring the shape.

A comparison of the observed signal with the expected signal in each channel provides a second check on the constancy of the pulse shape. The expected number of counts, m, is determined from the master pulse shape. In the absence of shape variations, the observed number of counts, n, should be Poisson distributed with mean m. For large m, the quantity $(n - m)/\sqrt{m}$ is approximately normally distributed with mean 0 and unit variance. The distribution of $(n - m)/\sqrt{m}$ for the 1969–1970 data is shown in the lower portion of figure 1. Also shown is the expected distribution for $m = 100$ (typical of the number of counts per channel). Again, the agreement between the observed and expected distributions indicates that systematic variations in the pulse shape are smaller than our measurement statistics.

Stricter limits can be established for long-term variations in the pulse shape. One might suppose, for example, that a change in the pulse shape would be associated with the frequency jump observed in 1969 September. To investigate this possibility, a pulse shape was constructed from all the data obtained in 1969 August and September, and a second pulse shape was constructed from an approximately equal amount of data obtained in 1969 October. The two shapes, along with their difference are shown in figure 2. It can be seen that there are no statistically significant (>3 percent) differences between the two shapes.

IV. REDUCTION TO BARYCENTRIC ARRIVAL TIMES

The location of the NP 0532 pulse in the CAT memory, the known time delays, and the starting time of the run are combined to yield a local time of arrival as in Boynton *et al.* (1969*a*).

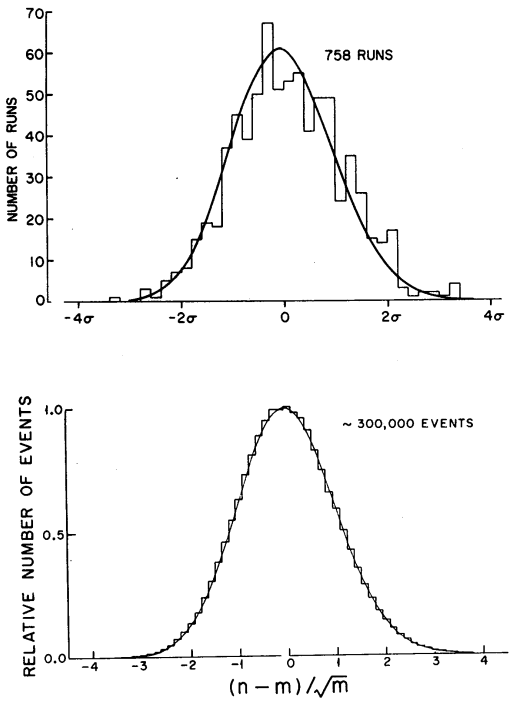

FIG. 1.—*Top*, histogram of the χ^2 distribution obtained when fitting the master pulse shape to the individual runs. *Bottom*, the distribution of $(n - m)/\sqrt{m}$ obtained by the same procedure. The curve in both figures is the expected distribution.

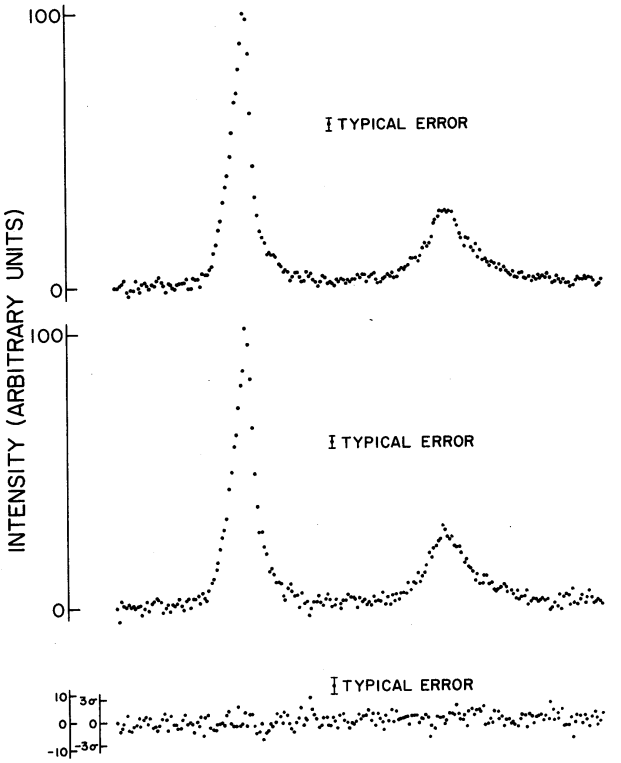

FIG. 2.—*Top*, average pulse shape of 1969 October. *Middle*, average pulse shape of 1969 August and September. *Bottom*, difference.

The local times of arrival are converted to barycentric times of arrival with the aid of the Jet Propulsion Laboratory Development Ephemeris 69. The planetary mass values used in these calculations are those recommended by JPL (O'Handley, Holdridge, and Mulholland 1969). The 1950.0 coordinates of NP 0532 have been taken to be those given by Minkowski (1966) and have not been corrected for proper motion (Trimble 1968).

The periodic gravitational redshifts and second-order Doppler shifts produced by the Earth's eccentric orbital motion (Hoffman 1968) are removed from the data by adding to each arrival time the term $(t - s)$, where t is coordinate time as measured by distant clocks and s is proper time as measured by Earth clocks. A numerical integration was performed with the aid of the JPL ephemeris to obtain $(t - s)$ as a function of s. The integration includes the effects of all the planets and the Moon as well as the Sun.

The gravitational path delay effect (Shapiro 1964) has been removed by adding to each time of arrival the term $(4r_0/c) \log (\cos \frac{1}{2}\theta)$, where r_0 is the gravitational radius of the Sun, c is the velocity of light, and θ is the angle subtended at the Sun by the Earth and NP 0532.

The 10 to 20 times of arrival obtained with a single night's observation are coherently combined into an average time of arrival. The errors which are independent from one run to the next are included in the averaging process and are therefore reduced by $\sim\sqrt{N}$, where N is the number of measurements in the average. Afterwards, the systematic errors are added quadratically and thus are not reduced by $\sqrt{N}$. Also, each average arrival time is unambiguously assigned a cycle number, beginning with 1 for the first pulse of 1970.

Over the 2-year observation period, 175 nightly barycentric times of arrival, together with cycle numbers and error estimates, have been obtained. The reduction of the error estimates over the observation period reflects improvements in instrumentation. Starting with 1969 August, the errors are dominated either by the 10-μs uncertainty in the Loran pulse phase or by counting statistics, depending on the quality and number of runs obtained on that night. Typically these errors range from 12 to 20 μs.

The error estimates do not include possible errors arising from the ephemeris corrections. Uncertainties in the pulsar position, the astronomical unit, and the orientation of the planetary and stellar coordinate systems appear to be the most likely possibilities for errors in the ephemeris corrections. However, each of these effects will lead to a spurious sinusoidal variation in the arrival times with an amplitude of several hundred microseconds and a period of 1 year. As will be seen in § V, NP 0532 appears to possess an intrinsic broad-band noise source with a 1-year component of several milliseconds amplitude. Thus, for the present, errors in the ephemeris corrections may be safely ignored.

It is important also to recognize that for the interpretation of long-term effects (timescales greater than 1 month) the noise component introduces uncertainties greater than our measurement errors. More accurate data are helpful only in analyzing effects of shorter time scale.

The Arecibo group has generously supplied 32 local arrival times to help fill in the 1969 summer gap in our data (Richards *et al.* 1970). The radio arrival times have been processed with our ephemeris, and a correction has been included to account for the observed variable dispersion measure (Rankin and Roberts 1970). Because of a difference in the definition of phase, 215 μs have been subtracted from all the Arecibo arrival times. The errors assigned to these data are those given by Arecibo.

V. ANALYSIS AND INTERPRETATION

a) Introduction

In attempting to interpret the barycentric arrival times in terms of models for the time dependence of the pulse frequency of NP 0532, we simply compare the phase of

the pulse, as predicted by the models, to the observed pulse phase. The phase is predicted by some function, $f(t, a_1, a_2, \ldots, a_m)$ of the time, t, and m adjustable parameters $a_1, a_2, \ldots, a_m$. If there are N barycentric arrival times, then the χ^2 of a given model is

$$\chi^2 = \sum_{i=1}^{N} [n_i - f(t_i, a_1, a_2, \ldots, a_m)]^2/\sigma_i^2 . \quad (1)$$

In equation (1), t_i is the ith arrival time, n_i is its associated cycle number, and $\sigma_i^2 = \nu^2 s_i^2$ where s_i^2 is the estimated variance in t_i and ν is the pulse frequency. In other words. t_i is the independent variable and n_i is the dependent variable with variance σ_i^2. To estimate the parameters a_j, the χ^2 is simultaneously minimized with respect to all the parameters.

After performing a fit we may compare the goodness-of-fit parameter, the χ^2, with its expected value, to see how well the model was able to predict the observed pulse phase. The residuals of the observations from the fitted function are also examined for systematic behavior not modeled in the fit.

Using the above procedure, we have been unable to find any simple function that produces a good fit. Furthermore, the residuals do not appear to be random, but show night-to-night correlations. That is, if a given night has a large residual, adjacent nights are likely to have a comparably large residual. Almost any 1-month-long string of data can be fitted reasonably well by a cubic polynomial. However, as soon as the data length exceeds the "fit threshold," i.e., 1 month, more and more parameters must be included in the fit in order to produce reasonable residuals. In fact, the number of parameters required appears to grow as N/a where N is the number of data points included in the fit and a is a number on the order of 2–4. Also, as noted by Papaliolios *et al.* (1970), it is only the *number* of parameters which seems to be important; the type of parameter does not seem to matter. One may produce comparable fits with high-order polynomials, discontinuously changing low-order polynomials, sinusoidal terms, etc. With a data length of the order of 1 year, an inordinately large number of parameters (20–30) is required. Furthermore, fits with large numbers of parameters have no predictive power. These fits cannot predict the phase either forward or backward in time any better than fits with only a few parameters.

There does, however, seem to be a persistent feature which stands out in these data. If one tries only fits to a cubic polynomial, then the residuals show a systematic behavior, the character of which does not depend either on the length of the data or which particular piece of data is included in the fit. The residuals show a quasi-sinusoidal behavior. The amplitude appears to grow with the length of the data, while the wavelength is one-third to two-thirds the length of the data. Note that a sinusoidal term with wavelength equal to the length of the data would, depending on the phase, be quite effectively removed by the cubic polynomial or else distorted into a quasi-sinusoidal term with a wavelength about two-thirds the length of the data. It is tempting to suppose that this behavior is present at all levels, including times less than 1 month. The existence of the fit threshold can be understood as the length of data below which the amplitude of the quasi-sinusoidal terms becomes unimportant compared with the measurement errors. The consistent appearance of this quasi-sinusoidal term will be important in § V*d*, where a noise model is developed in an attempt to understand this characteristic structure of the data.

In the model presented below it will be assumed that the pulsar has an intrinsic source of noise which is superposed upon the overall cubic braking polynomial. The idea that a definite functional form could be found was not abandoned lightly. Much effort was spent in trying to obtain good fits to a variety of functions. For example, at one point a 19-parameter fit was obtained which seemed to fit most of the 1969–1970 data reasonably well. In this particular fit, it was assumed that the pulsar had three

orbiting companions. The 19 parameters included five parameters for each orbiting companion, as well as four parameters for the cubic polynomial. It should be noted that the effects of orbiting companions similar to the inner planets of the solar system would be quite easy to see in these data. A time-of-arrival measurement with an accuracy of 10 μs is also a measure of the relative distance between the Earth and the pulsar to an accuracy of about 2 miles. In any event, the three-planet fit was unable to predict the phase during the 1970–1971 observing season. Rather than add more and more planets as more and more data were obtained, the planetary hypothesis was abandoned. The many other functions that were tried met the same fate.

In addition to the cubic polynomial and the noise source, the model must also include some kind of function to account for the speedup, or glitch, which occurred in 1969 in late September. As far as the glitch is concerned, the greatest success has been obtained with the four-parameter "glitch function" derived from the two-component model suggested by Ruderman (1969) and developed by Baym *et al.* (1969). The glitch is discussed in greater detail in § V*c*.

b) *Cubic Polynomial*

By far the largest effect present in the data is the cubic polynomial, which accounts for the secular slowing down of the pulse frequency. Why should we expect a cubic polynomial? Theoretical papers have predicted that ν and $\dot{\nu}$ should satisfy the relation

$$\dot{\nu} = K\nu^n , \tag{2}$$

where n, the braking index, and K are constants for simple models. The exact value of n depends on the mechanism responsible for loss of angular momentum in the pulsar. A braking mechanism of the "solar wind" type would give $n = 1$ (Michel and Tucker 1969), while braking by pure (magnetic) dipole radiation would yield $n = 3$ (Pacini 1967; Gunn and Ostriker 1969; Ostriker and Gunn 1969), and braking by pure (gravitational) quadrupole radiation would yield $n = 5$ (Ferrari and Ruffini 1969), etc.

Differentiation of equation (2) produces simple relations between n and the higher derivatives of the pulse frequency,

$$\ddot{\nu} = n\dot{\nu}^2/\nu , \tag{3}$$

$$d^3\nu/dt^3 = (2n^2 - n)\dot{\nu}^3/\nu^2 . \tag{4}$$

Using the known values of ν and $\dot{\nu}$, 30 Hz and -4×10^{-10} Hz s^{-1}, and assuming that n is in the range 1–5, one finds that the cubic term in the pulse phase becomes 20–100 cycles after 1 year. Such an effect is easily observable. On the other hand, the quartic term would be only -0.002 to -0.1 cycles after 1 year. Were NP 0532 to follow only a simple slowing-down law, such an effect might be observable. As it is, the presence of other effects makes the term completely unobservable.

Figure 3 shows the residuals from cubic polynomial fits to all the data, and the two halves of the data. It should be kept in mind that these plots merely show the difference between time as kept by the pulsar clock and the time shown by a fictitious clock that keeps time according to the fitted function. A positive residual indicates that the pulsar was ahead of the fitted clock, i.e., the pulse arrived earlier than expected.

The characteristic quasi-sinusoidal behavior can be seen in these plots. Also, the frequency jump of 1969 late September stands out. Figure 4 shows the residuals from cubic fits to the four quarters of the data. Again, the quasi-sinusoidal behavior can be seen, although the period and amplitude are considerably reduced. It should be noted that neither the amplitude nor the phase repeats from one segment of the data to the next. The sinusoidal term reported by Arecibo can be seen in figure 4 (Richards *et al.* 1970), although the addition of data for 1969 March and April alters the period and amplitude from 77 to 100 days and from 380 to 500 μs.

1972ApJ...175..217B

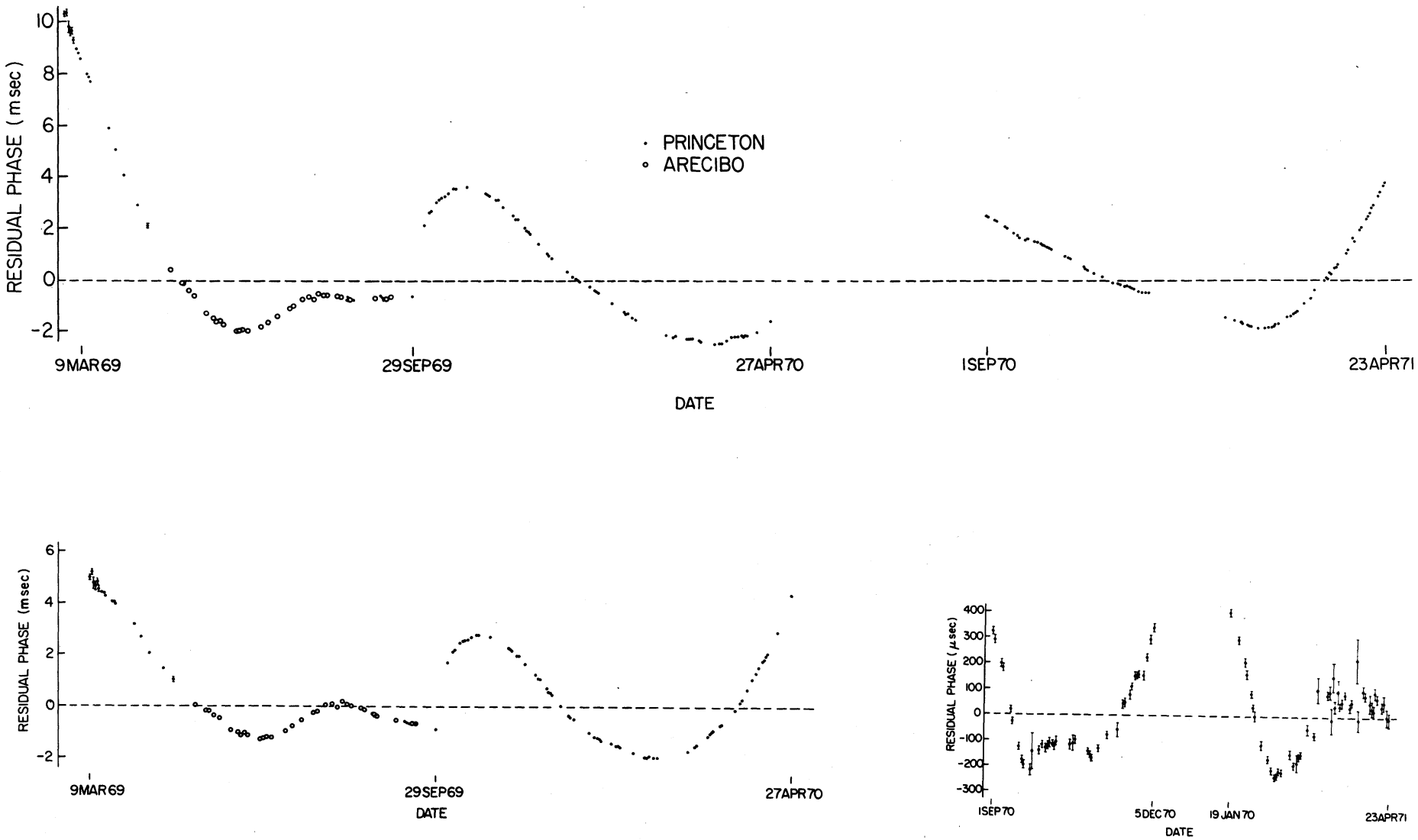

FIG. 3.—*Top,* residuals from a cubic fit, 1969 March 9–1971 April 23. *Bottom left*, cubic residuals, 1969 March 9–1970 April 27. *Bottom right*, cubic residuals, 1970 September 1–1971 April 23.

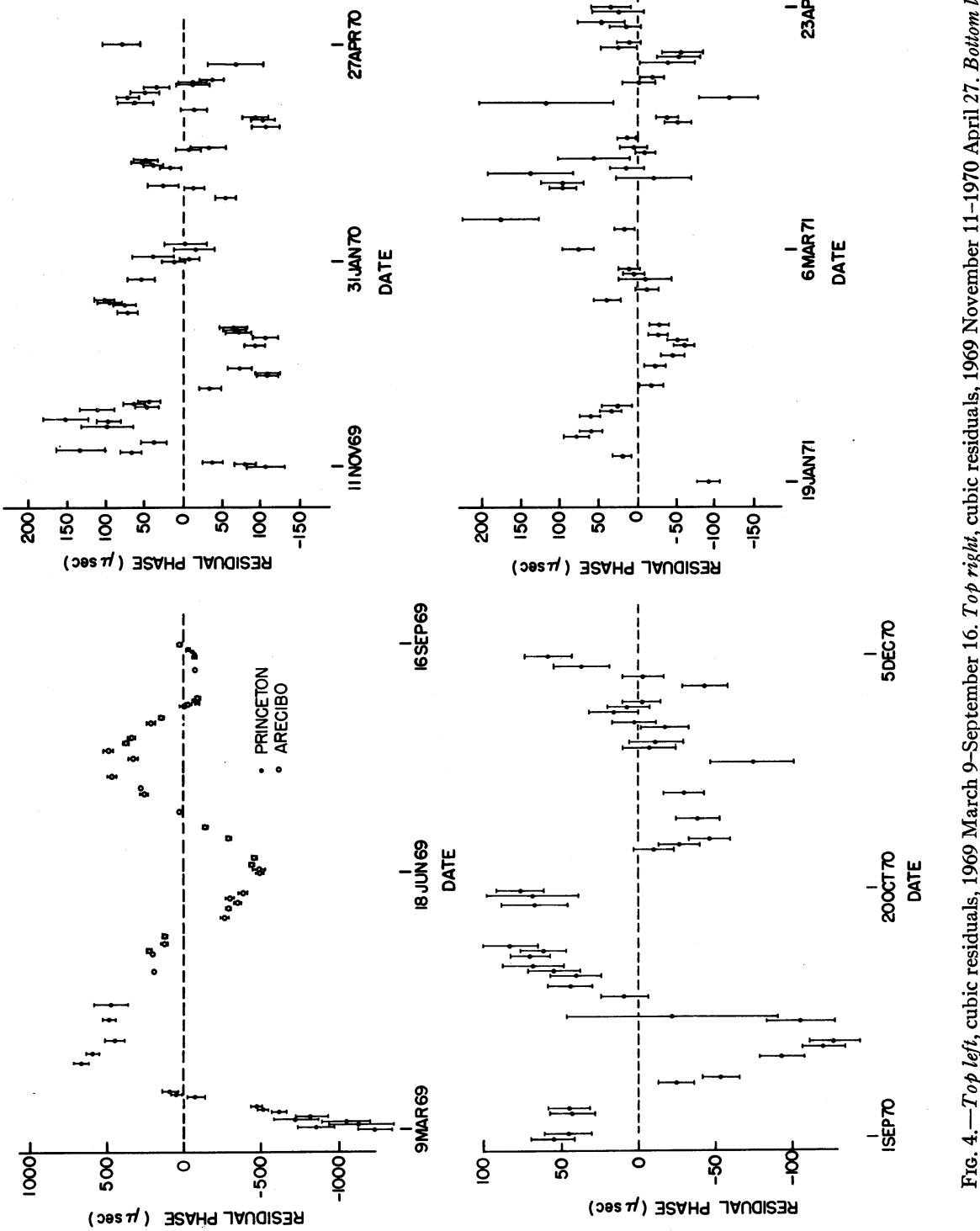

FIG. 4.—*Top left*, cubic residuals, 1969 March 9–September 16. *Top right*, cubic residuals, 1969 November 11–1970 April 27. *Bottom left*, cubic residuals, 1970 September 1–December 5. *Bottom right*, cubic residuals, 1971 January 19–April 23.

TABLE 1

CUBIC POLYNOMIAL PARAMETERS

Time Span	χ^2/N	ϕ_0(Cycles)	ν_0(Hz)	$\dot{\nu}_0(10^{-10}$ Hz $s^{-1})$	n
1969 Mar. 9–1971 Apr. 23.....	2375000/207	0.78177(6)	30.205865616586(4)	−3.856004015(5)	2.514826(8)
1969 Mar. 9–1970 Apr. 27.....	781300/122	0.82043(8)	30.205865613232(9)	−3.85603013 (3)	2.45039 (8)
1970 Sept. 1–1971 Apr. 23.....	8356/85	−0.898 (9)	30.2058658326 (9)	−3.8561750 (6)	2.6439 (4)
1969 Mar. 9–1969 Sept. 16....	10170/56	0.328 (3)	30.2058655065 (7)	−3.8561826 (9)	2.237 (1)
1969 Nov. 11–1970 Apr. 27.....	878/54	0.7893 (1)	30.20586559665 (3)	−3.8559879 (2)	2.589 (1)
1970 Sept. 1–1970 Dec. 5.....	471/39	0.5 (1)	30.20586569 (1)	−3.85607 (1)	2.576 (8)
1971 Jan. 19–1971 Apr. 23.....	295/46	15.5 (4)	30.20586453 (3)	−3.85548 (2)	2.272 (9)

NOTE.—Numbers in parentheses are the error in the last digit.

It is reasonable to ask whether the large residuals occurring in figures 3 and 4 are due to measurement errors rather than the intrinsic behavior of the pulsar. Every statistical test performed on these data or on the data used in the construction of the ephemeris indicates that the error assignments are consistent with the actual measurement errors. In addition, the four groups performing optical time-of-arrival measurements during the period 1969 December–1970 April have compared the four independent sets of data obtained during this period (Horowitz *et al.* 1971). The comparison indicated that the data agree to within the assigned errors.

The parameters associated with the fits of figures 3 and 4 are collected in table 1. The unit of time used in table 1 is the Universal Time second, while t_0 has been chosen as 0^h UTC 1970 January 1. The errors given are purely formal errors derived from the errors associated with the individual measurements. The quoted errors do *not* reflect the fact that the quality of the fits is so poor.

The braking index seems to hover around 2.5, although there is considerable variance in the values given in table 1. Of course, one interpretation of this large variance is that the braking index is a time-dependent parameter and the values in the table reflect this time dependence. In view of the results to be presented in § V*d*, we feel that a more reasonable interpretation is that the true value of the braking index is distorted by the noise component in the data. Perturbations of n introduced by phase and frequency noise have zero mean. Slowing-down noise would alter the mean braking index, but only by a negligible amount. Thus, as one includes more data in the fit, the fitted value of the braking index should "zero in" on the correct value.

It is clear from the values listed in table 1 that 2 years of data is not sufficiently long for the convergence to have occurred. To obtain a best measure for the braking index, we have calculated the average value of n from the fits presented in figure 4. All these fits include about the same amount of data, so the variance due to the noise component in each individual value is approximately the same. We find

$$n = 2.42 \pm 0.22 . \quad (5)$$

The error given in equation (5) is the 90 percent confidence interval, if the four samples are assumed to be statistically independent.

The value of the braking index obtained here is not consistent with either 1, 3, or 5, as predicted by simple models of the pulsar radiation mechanism. We emphasize, however, that an underlying braking mechanism with a time-independent n is consistent with these data if a noise component is indeed present.

c) *Frequency Jump*

The NP 0532 frequency jump of 1969 late September (Boynton *et al.* 1969*b*; Richards *et al.* 1969) was much smaller than that observed in the Vela pulsar (Radhakrishnan and Manchester 1969; Reichley and Downs 1969) and apparently has a much shorter recovery time. Several models have been proposed to explain the occurrence of these glitches. The periapsis passage of an orbiting companion of the pulsar has been suggested by Michel (1970) and by Hills (1970). One would expect that frequency jumps of both signs should occur if this model were the correct explanation; the events so far observed have been increases in frequency. A stronger argument can be made with the data themselves. Figure 5 shows the results of fitting a cubic polynomial to the data immediately preceding the glitch. The data after September 29 have not been included in the fit. The residuals shown in figure 5 are the result of extrapolating the fitted function to the data beyond the glitch. Of course, one cannot extrapolate very far before the errors in the cubic polynomial become important. However, an extrapolation of a few weeks should be reasonably safe. In the week between 1969 September 29 and October 6, the pulsar gained about a tenth of a cycle in phase. Thereafter, the phase gain slowed down. A model based on the close passage of an orbiting companion cannot fit the curvature between October 6 and October 16, and at the same time fit the sharp break between September 29 and October 6. In fact, we were unable to find any smooth function which would fit the data near the glitch. For example, we have tried arc-tangent functions and error functions without success.

So far, the model which has been most successful in fitting the data near the glitch is the two-component starquake model proposed by Ruderman (1969), and applied to glitches by Baym *et al.* (1969). In this model the pulsar is envisioned as a neutron star with a superfluid core and a solid crust. The pulses are assumed to originate from a region that rotates with the crust, and the braking torque is applied to the crust. Because the core is superfluid, the crust-core coupling is extremely weak—the characteristic relaxation time is of the order of days to years, depending on the mass of the star. At the time of the glitch, something causes the crust to speed up. In the model developed by Baym *et al.* (1969), the speedup is due to a cracking and shrinking of the crust. Other workers have suggested that the speedup may be due to an instability in the crust-core coupling (Greenstein and Cameron 1969). In any event, after the speedup occurs, the crust slowly communicates its excess speed to the core, causing the core to speed up and the crust to slow down.

If t_g is the glitch time, then the glitch function predicted by the model above is zero for $t < t_g$, and for $t > t_g$ one has

$$\Delta\phi = \Delta\nu[[Q\tau\{1 - \exp[-(t - t_g)/\tau]\} + (1 - Q)(t - t_g)]] . \quad (6)$$

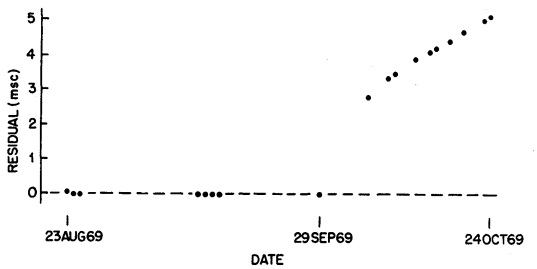

FIG. 5.—Residuals from a cubic fit. Only the data before 1969 September 29 were included in the fit.

In this expression, $\Delta\phi$ is the excess phase produced by the glitch, $\Delta\nu$ is the instantaneous frequency jump at the time of the glitch, τ is the relaxation time of the crust-core coupling, and Q is the fraction of the moment of inertia carried by the core in the two-component model ($0 < Q < 1$). Large Q means that most of the initial speedup of the crust decays away by transferring angular momentum to the massive core, thus slowing down the crust which presumably controls the pulse rate. On the other hand, small Q means that very little of the initial speedup decays. Also, small Q indicates a light neutron star, while large Q indicates a more massive neutron star.

Figures 6–8 show the residuals from fitting a cubic polynomial and a glitch function to the data near the glitch. The different fits include successively larger pieces of data.

The glitch parameters generated by these fits are collected in table 2. Again, the errors given are formal errors and so do not reflect the quality of the fit; this is indicated by χ^2/N. The values of several of the parameters show interesting correlations with the length of the data string used in the fit. For example, the relaxation time starts at about 4 days and increases to about 20 days as the length of the data string increases from 52 to 414 days. Similarly, Q starts at about 0.9 and increases to 2. The instantaneous change in frequency decreases from 2.8×10^{-7} Hz to 0.8×10^{-7} Hz; the χ^2/N increases drastically.

What are the implications of these correlations? We believe that as the data length becomes longer, the noise components become more important (as expected from the power spectrum), and a compromise is made between fitting the glitch and fitting the noise component. Except for the residual change in frequency (last term in eq. [6]), the glitch function affects only those points within a few relaxation times of t_g.

For the short lengths of data, with τ about 4 days, the exponential part of the glitch has decayed to the level of the measurement errors after 2–3 weeks. For the longest lengths of data, when τ is about 2 weeks, the exponential term does not decay to the level of the errors for 3–4 months. In effect, the glitch function is trying to remove the large structure seen in figure 3 instead of the structure near the glitch. This can also be seen by comparison of figures 3 and 8. Even in figure 7 we see the noise components becoming important.

Clearly, it is not meaningful to force the glitch function to fit noise components. In § V*d* the noise component is modeled by fitting a Fourier series to the data. It will be shown that fitting a cubic polynomial, a Fourier series, and a glitch function to the data of figure 8 produces estimates of the glitch parameters quite similar to those produced by the fits of figure 6. Thus, we believe that the most reliable estimates of the glitch parameters are those estimated from short lengths of data (fig. 6 and the first two lines of table 2).

There is no well-defined procedure for assessing the uncertainties in these estimates.

TABLE 2

GLITCH PARAMETERS

Time Span	χ^2/N	$\Delta\nu$ (10^{-7} Hz)	τ (days)	Q	t_g − 1969 Sept. 29 (hours)
1969 Aug. 23–Oct. 24	24/23	2.86±0.52	4.1±1.1	0.934±0.026	20.8±7.7
1969 Aug. 23–Nov. 21	72/30	2.49±0.07	4.7±0.2	0.897±0.008	7.4±4.4
1969 July 21–Dec. 20	1250/50	2.18±0.02	7.7±0.1	0.943±0.003	− 4.5±2.8
1969 Feb. 1–1970 Feb. 1	3470/69	1.58±0.01	15.2±0.1	1.151±0.004	−12.2±3.5
1969 Mar. 9–1970 Apr. 27	75500/122	0.77±0.02	19.6±0.2	1.937±0.021	52.2±5.4

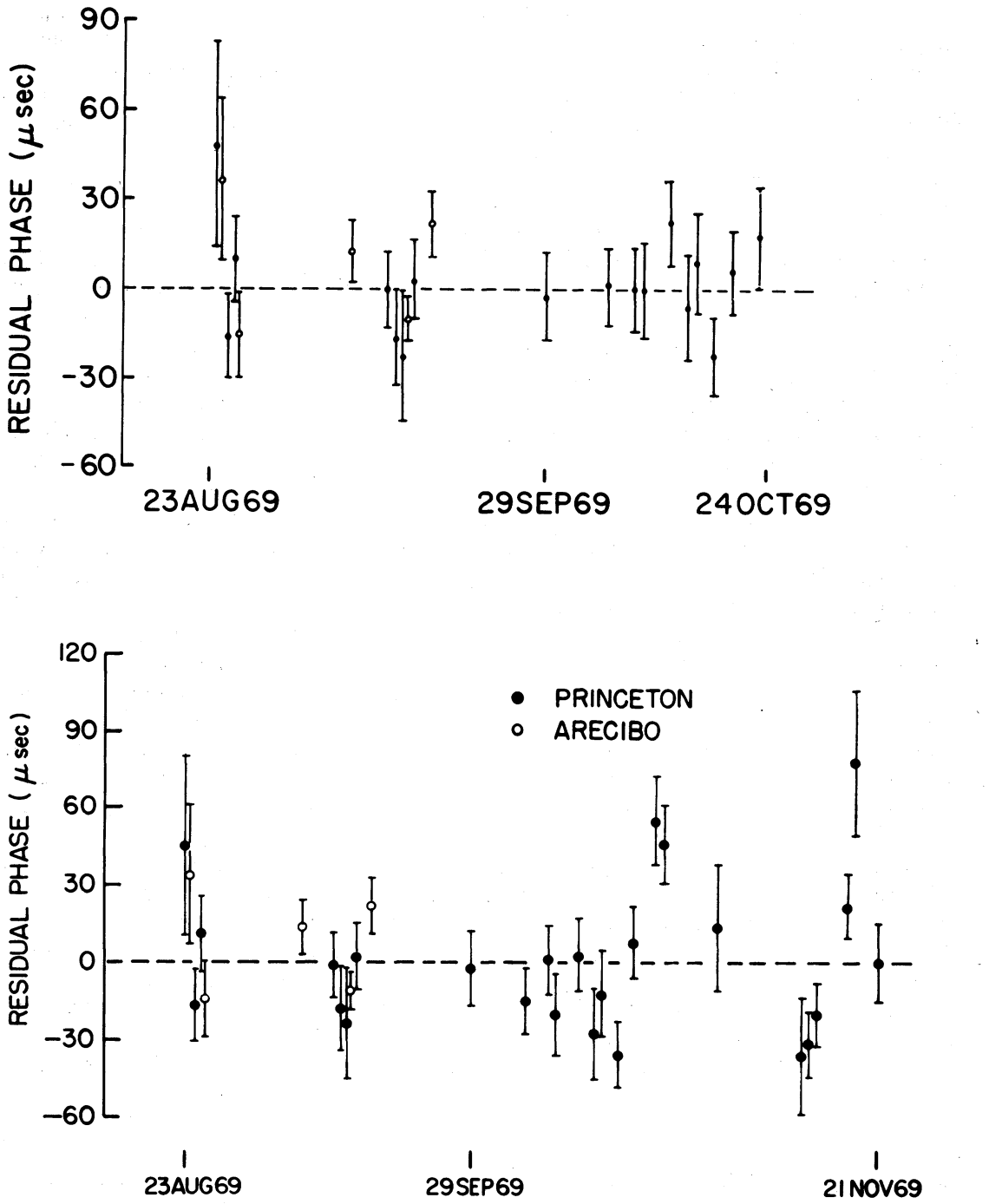

FIG. 6.—Residuals from a cubic polynomial and a glitch function. *Top*, 1969 August 23–October 24. *Bottom*, 1969 August 23–November 21.

We adopt a conservative procedure using the parameter estimates obtained from the shortest fits (fig. 6) as upper and lower limits on the values of the parameters. In addition, one must allow for the errors in these estimates. The χ^2 for the shortest fit shown in figure 6 is only 24 for 15 degrees of freedom. Thus, the error estimates obtained from this fit are probably too small by at most a factor of 1.3. To be on the conservative side,

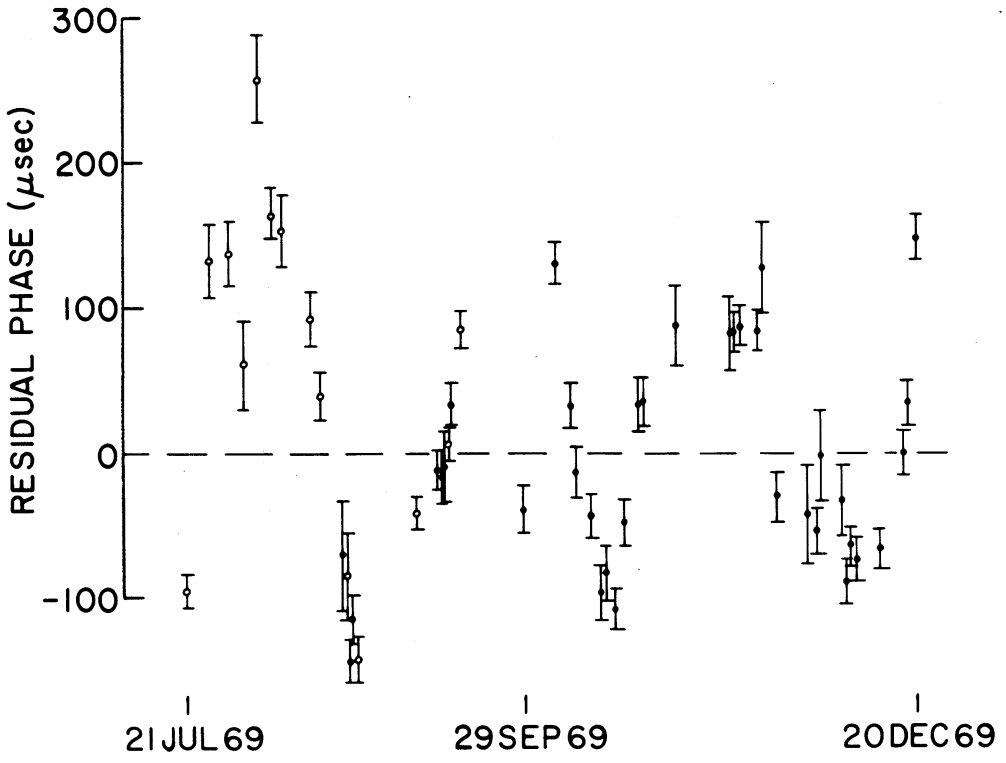

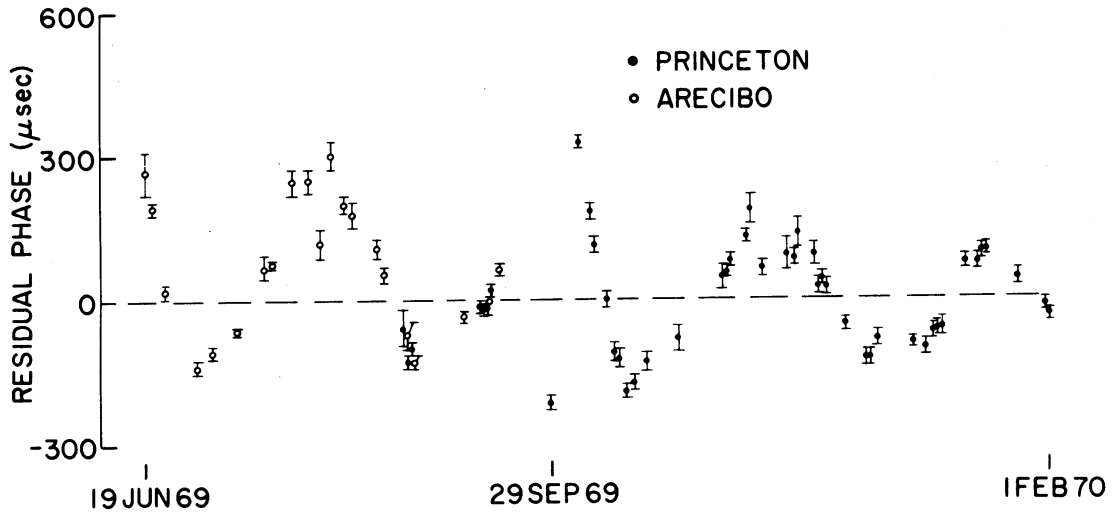

FIG. 7.—Residuals from a cubic polynomial and a glitch function. *Top*, 1969 July 21–December 20. *Bottom*, 1969 June 19–1970 February 1.

the upper and lower limits have been widened by twice these error estimates. The limits defined by this procedure are

$$1.5 \times 10^{-7} \leq \Delta\nu \leq 3.8 \times 10^{-7} \quad \text{(Hz)}, \quad (7)$$

$$2.8 \leq \tau \leq 6.9 \quad \text{(days)}, \quad (8)$$

$$0.85 \leq Q \leq 0.996, \quad (9)$$

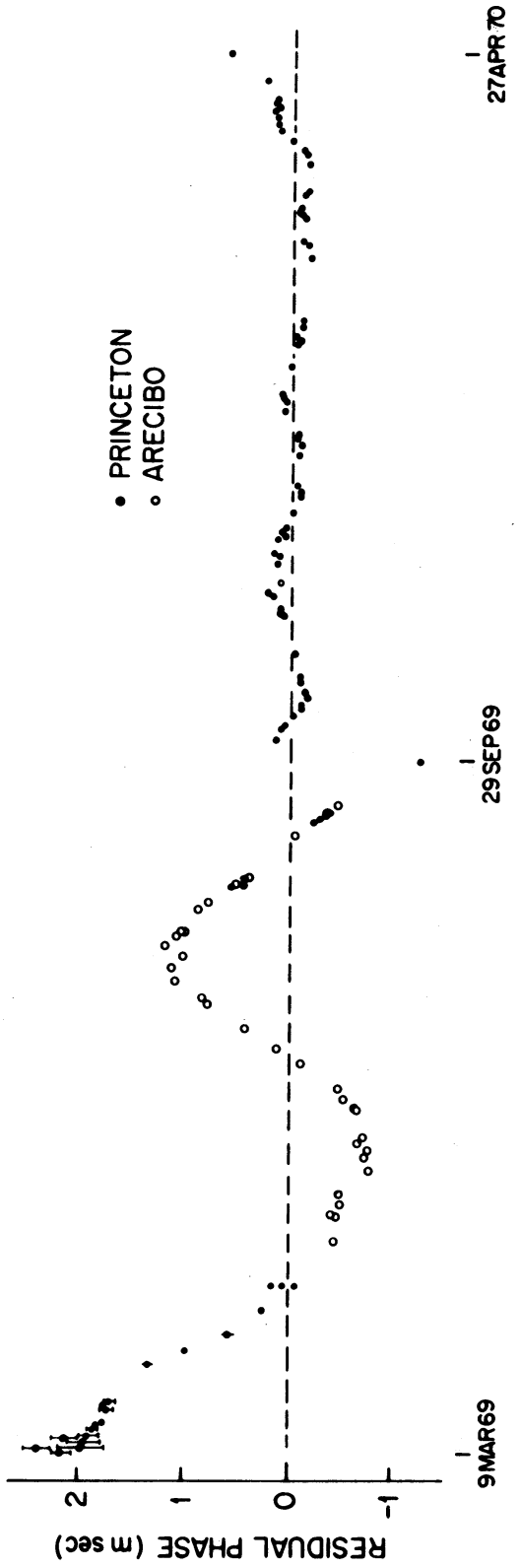

FIG. 8.—Residuals from a cubic polynomial and a glitch function, 1969 March 9–1970 April 27

and $$-8 \leq t_g \leq 36 \quad \text{(hours)} . \quad (10)$$

The glitch time t_g is measured in hours from 0^h UTC 1969 September 29.

The value of Q given in equation (9) does not agree with the value 0.34 obtained by Papaliolios *et al.* (1970). However, they had no data between 1969 September 16 and 1969 October 9. In addition, they obtained Q from a formula involving the changes in the cubic polynomial parameters, but that formula is applicable only if the relaxation time is long compared to observation time; we believe this not to be the case.

The results obtained in equations (7)–(10) may be used to draw conclusions about the structure of the pulsar. If the two-component model is the correct interpretation of the glitch, then the lower limit of 2.8 days for the relaxation time is direct experimental evidence that the neutrons and protons in the neutron-star core are in a superfluid state. Otherwise, the crust-core coupling would be too strong, and the relaxation too fast to observe (Baym *et al.* 1969). Also, an estimate of Q may provide a measure of the neutron-star mass. According to current models, a relatively thin crust (large Q) implies high mass—probably greater than 0.6 $M_\odot$ (Baym and Pines 1971).

d) Noise Components

As noted in § V*a*, a persistent feature of the data is the quasi-sinusoidal structure that appears in residuals whenever more than a month of data are fitted with a cubic polynomial. The characteristics of these residuals, and our failure to find definite functions with predictive power, lead us to propose a noise component connected with the clock mechanism of NP 0532.

Following Groth (1971), three simple noise models are considered: "phase noise," "frequency noise," and "slowing-down noise." In each of these models, the pulsar is assumed to follow exactly a power-law slowdown as in equation (2), except that at random times the pulse phase, frequency, or slowing-down rate jumps, or changes discontinuously. That is, one of the three parameters ϕ, ν, or $\dot{\nu}$ is undergoing a random walk. It is assumed that the size of the jumps is randomly distributed, that the distribution of jump sizes possesses both a first and second moment, and that all jumps are independent. The statement that events occur at random times means that in time intervals of length T, the number of events follows a Poisson distribution with mean RT, where R is the average number of jumps per unit time. Actually, it will not be necessary that both the times and the amplitudes of the events be random; either one will do. For generality, however, the models are developed as if both are randomly distributed. The final assumption is that the noise process is stationary; that is, neither the amplitude distribution nor the average rate depends on time. The glitch of 1969 September 29 will not be considered in the following discussion. It may in fact be a part of the noise process; but if so, it is far out on the tail of the amplitude distribution.

The first question to ask is: How do random events of this type affect the cubic parameters discuss in § V*b*? Split the phase into the overall slowing-down term and a random part,

$$\phi = \phi_S + \phi_R . \quad (11)$$

In this expression, ϕ_S is the secular part of the phase and is assumed to be given by equation (2). The random part of the phase is given by ϕ_R, which for the three kinds of noise is

$$\phi_R = \sum_{i=1}^{N} \Delta\phi_i H(t - t_i) \quad \text{(phase)} , \quad (12)$$

$$\phi_R = \sum_{i=1}^{N} \Delta\nu_i (t - t_i) H(t - t_i) \quad \text{(frequency)} , \quad (13)$$

and

$$\phi_R = \sum_{i=1}^{N} \tfrac{1}{2}\Delta\nu_i (t - t_i)^2 H(t - t_i) \qquad \text{(slowing down)} . \quad (14)$$

In these expressions, $H(t)$ is the unit step function at $t = 0$; $\Delta\phi_i$, $\Delta\nu_i$, and $\Delta\dot{\nu}_i$ are random variables giving the amplitude of the jumps; and t_i are random variables giving the times of the jumps. If one has data in blocks of length T, then N is also a random variable whose mean is RT. All the $\Delta\phi_i$, $\Delta\nu_i$, or $\Delta\dot{\nu}_i$; t_i; and N are assumed to be independent.

If a cubic polynomial is fit to $\phi_S + \phi_R$, the parameters will be perturbed from those of ϕ_S by the noise component. The average values of the parameter perturbations may be obtained from the average of ϕ_R, since each parameter is a linear function of ϕ_R. This average is calculated by averaging over the $\Delta\phi_i$, $\Delta\nu_i$, or $\Delta\dot{\nu}_i$ distribution, the t_i distribution, and the N distribution, which yields

$$\langle\phi_R\rangle = \langle\Delta\phi\rangle RT \qquad \text{(phase)} , \quad (15)$$

$$\langle\phi_R\rangle = \langle\Delta\nu\rangle RT^2/2 \qquad \text{(frequency)} , \quad (16)$$

$$\langle\phi_R\rangle = \langle\Delta\dot{\nu}\rangle RT^3/6 \qquad \text{(slowing down)} . \quad (17)$$

In these expressions $\langle\Delta\phi\rangle$, $\langle\Delta\nu\rangle$, and $\langle\Delta\dot{\nu}\rangle$ are the first moments of the $\Delta\phi_i$, $\Delta\nu_i$, and $\Delta\dot{\nu}_i$ distributions. On the average, each kind of noise will produce an offset in one of the polynomial parameters of ϕ_S.

We may also calculate the dispersion in the cubic parameters. In particular, the standard deviation of $\ddot{\nu}$ is given by,

$$\langle\Delta\ddot{\nu}^2\rangle^{1/2} = 2946[R\langle\Delta\phi^2\rangle]^{1/2}/T^{5/2} \qquad \text{(phase)} , \quad (18)$$

$$\langle\Delta\ddot{\nu}^2\rangle^{1/2} = 5.1[R\langle\Delta\nu^2\rangle]^{1/2}/T^{3/2} \qquad \text{(frequency)} , \quad (19)$$

$$\langle\Delta\ddot{\nu}^2\rangle^{1/2} = 1.8[R\langle\Delta\dot{\nu}^2\rangle]^{1/2}/T^{1/2} \qquad \text{(slowing down)} . \quad (20)$$

In these expressions, $\langle\Delta\phi^2\rangle$, $\langle\Delta\nu^2\rangle$, and $\langle\Delta\dot{\nu}^2\rangle$ are the second moments of the jump amplitude distributions. The expressions are valid only if a cubic polynomial is fitted.

The different dependence on T in equations (18), (19), and (20) can be used to discriminate between kinds of noise. Dividing their data into four 1-month-long segments, the Lick group found values of n ranging from 0 to 4 (Nelson *et al.* 1970). This implies a dispersion in $\ddot{\nu}$ of about 10^{-20} Hz s^{-2}. With a data length of about 5 months, the dispersion in $\ddot{\nu}$ is about 0.1×10^{-20} Hz s^{-2} (see eq. [5]).

If one writes

$$\Delta\ddot{\nu}_1/\Delta\ddot{\nu}_2 = (T_1/T_2)^{\alpha} , \quad (21)$$

then α is -1.4. This is a strong indication that the noise component is predominantly frequency noise, since the dispersion is dying out as predicted by equation (19). Furthermore, $R\langle\Delta\nu^2\rangle$ can be estimated as

$$R\langle\Delta\nu^2\rangle \approx 9 \times 10^{-23}\ \text{Hz}^2\ \text{s}^{-1} , \quad (22)$$

giving a rough value suitable for the testing of physical models.

Another method of studying a noise process is to study its power spectrum. With methods similar to those described by Rice (1954) the power spectra expected from the three kinds of noise are calculated to be

$$P(\omega) = 2R\langle\Delta\phi^2\rangle/\omega^2 \qquad \text{(phase)} , \quad (23)$$

$$P(\omega) = 2R\langle\Delta\nu^2\rangle/\omega^4 \qquad \text{(frequency)} , \quad (24)$$

$$P(\omega) = 2R\langle\Delta\dot{\nu}^2\rangle/\omega^6 \qquad \text{(slowing down)} , \quad (25)$$

where $P(\omega)$ is the power per hertz at frequency ω.

The power spectra of our time-of-arrival data have been obtained by simultaneously fitting a cubic polynomial and a Fourier series to the data. The Fourier series is

$$\phi_{\rm FS} = \sum_{n=1}^{10} \left(a_n \cos \frac{2\pi n}{T} t + b_n \sin \frac{2\pi n}{T} t \right). \tag{26}$$

The period of the fundamental component, T, is taken to be about 90–95 percent of the length of the data in order to reduce interference with the cubic polynomial. The series is truncated at 10 terms because higher-frequency terms have periods which approach the size of the gaps in the data. In addition to the cubic polynomial and a Fourier series, the fit includes the glitch function (eq. [6]) when appropriate.

Letting $c_n^2 = a_n^2 + b_n^2$, one has

$$c_n^2/2 = P(\omega)/T\,, \tag{27}$$

where T^{-1} is the bandwidth factor. In figure 9 is plotted log c_n^2 versus log n for various segments of the data. The upper curve is from a fit to all the 1969–1970 data, and a glitch function was included in this fit. The lower curves are from fits to the 1969–1970 data before and after the glitch. Unfortunately, the 1970–1971 data with the large gap in the middle cannot be analyzed this way. The error bars in figure 9 have been drawn under the assumption that a_n and b_n are independent and normally distributed. They are not the errors obtained in the fit, which are much smaller. The best-fitting lines in which both the intercept and the slope are fitted are shown by the dashed lines. The solid lines show the best-fitting lines when only the intercept is allowed to vary and the slope is fixed at -4. By computing the variance of log c_n^2, one can show that 72 percent of the points should lie within their errors of the fitted lines. (In fact, 23/30, or 77 percent, lie within their error bars of the fitted lines.) Thus, it appears that the power spectra of these data are consistent with frequency noise, and another estimate (to within an order of magnitude) can be obtained for $R\langle \Delta\nu^2 \rangle$,

$$R\langle \Delta\nu^2 \rangle \approx 3 \times 10^{-22}\ {\rm Hz^2\ s^{-1}}\,. \tag{28}$$

Of course, in the plots of figure 9 problems due to end effects and the irregular distribution of the data have been ignored. These problems will be discussed in greater detail in the next section.

The fit used in obtaining the upper power spectrum in figure 9 included a glitch function. In this particular fit, the glitch function was not forced to fit the long-term structure that we attribute to noise—the Fourier series takes care of that. The glitch parameters obtained in this fit are

$$\Delta\nu = (2.2 \pm 0.4) \times 10^{-7}\ {\rm Hz}\,, \tag{29}$$

$$\tau = 4.4 \pm 0.7\ {\rm days}\,, \tag{30}$$

$$Q = 1.07 \pm 0.20\,, \tag{31}$$

which are consistent with the ranges in equations (7)–(10). The large error associated with Q arises because of large interference between the low-frequency components and the long-term behavior of the glitch function. For this reason, the estimate for Q given by equation (9) is probably more reliable than that given in equation (31).

e) Monte Carlo Approach

Although the straightforward power-spectrum analysis of the previous section provides quantitative support for the frequency-jump noise model, it gives us little intuitive insight into the general characteristics of the noise process. Also, there are some obscure

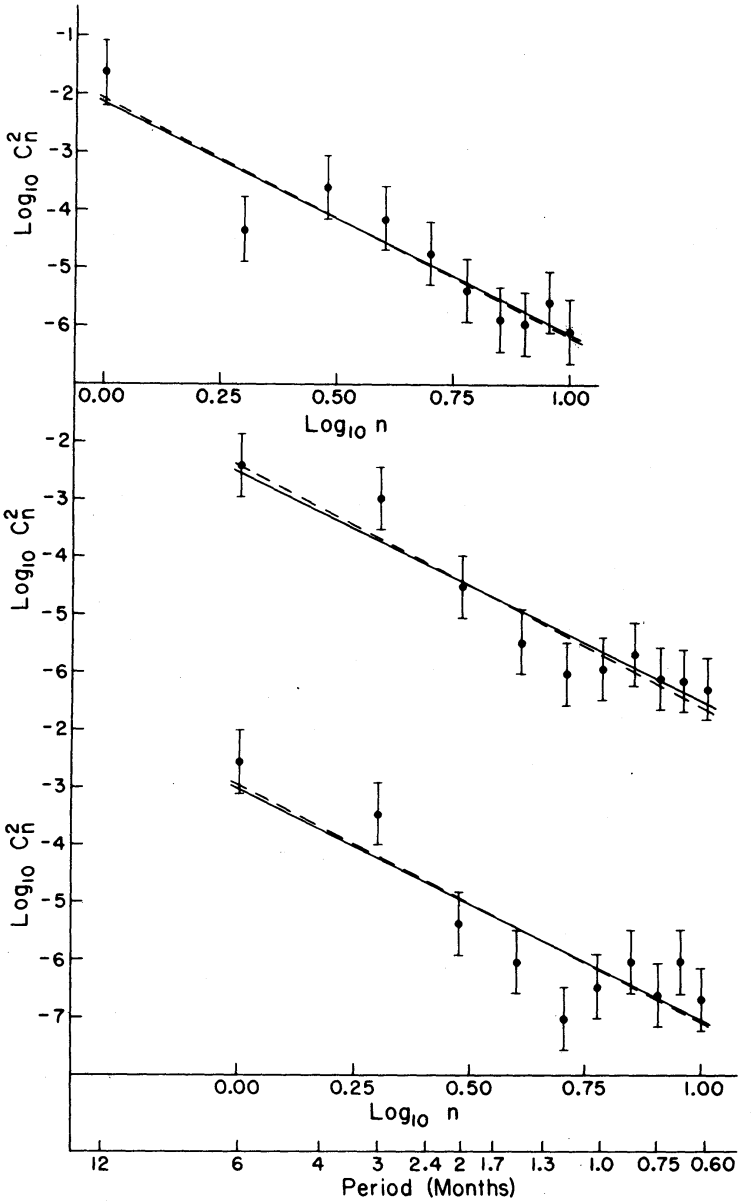

FIG. 9.—*Top*, power spectrum of the noise component in the 1969–1970 data. *Middle*, power spectrum of the pre-glitch data. *Bottom*, power spectrum of the post-glitch 1969–1970 data. *Dashed lines*, the best-fit lines when both height and slope are fitted. *Solid lines*, the best-fit lines with slope fixed at −4.

questions about the effects on our fitting procedure of (1) finite data strings, (2) irregular discrete sampling, and (3) interference between the cubic polynomial and the Fourier series functions. It was decided (Groth 1971) to construct data sets from our model functions, but with the noise component generated by random numbers with a computer. These pseudo-data were then subjected to our fitting and power-spectrum programs to see how accurately the model parameters could be recovered in the presence of random noise.

The pseudo-data are constructed as follows. First, a subset of the real data is chosen (in this case, all the data obtained after 1969 November 11), and the times of arrival are adjusted to produce a set of arrival times which conform exactly to a cubic polynomial.

Measurement error is simulated by adding to each arrival time a normally distributed random number having zero mean and standard deviation equal to the assigned error. Next, 2000 random numbers, t_i, are generated. These numbers are randomly distributed over the time interval containing the data. Finally, the perfect cubic data with measurement error and the ϕ_R, generated from equation (12), (13), or (14), are combined to produce three sets of pseudo-data. In the first set, a phase jump of 1.6×10^{-3} cycles is constructed at each t_i; in the second, a frequency jump of 2.3×10^{-9} Hz is constructed at each t_i; and in the third, a jump of 2.0×10^{-15} Hz s^{-1} in the slowing-down rate is constructed at each t_i. Many sets of pseudo-data were constructed so that a qualitative feeling of the characteristics of each kind of noise can be obtained. Note that these data sets (1) have the same sampling and weighting structure as the real data, (2) have the same measurement noise as the real data, (3) follow a cubic braking function as the real data are believed to do, and (4) contain a noise component of known strength (i.e., $\Delta\phi$, $\Delta\nu$, or $\Delta\dot{\nu}$; and R are chosen).

Quantitative results from fitting the pseudo-data indicate that our programs accurately recover function parameters (aside from the offsets given in eq. [15]–[17]) from our real data, even in the presence of noise. However, power spectra of the noise in the pseudo-data indicate a weakness in our ability to distinguish phase-jump noise from frequency-jump noise with our current data set. Power spectra proportional to $\omega^{-3.5}$, ω^{-4}, and ω^{-6} were obtained for computer-generated phase noise, frequency noise, and slowing-down noise, respectively. The data of figure 9 cannot distinguish between slopes of -3.5 and -4.

Qualitative results of the Monte Carlo procedure are shown in figures 10–15. Each figure shows the residuals from cubic polynomial fits to the real data and three sets of pseudo-data. The pseudo-data sets are not selected; they are the first three produced by the computer. Figures 10, 11, and 12 show phase noise, frequency noise, and slowing-down noise, respectively; figures 13, 14, and 15 show cubic fits to the first thirds of the data shown in figures 10–12.

Inspection of figure 10 shows that the phase-noise pseudo-data do not contain large enough low-frequency components, while figure 12 shows that the slowing-down-noise models are too smooth when compared with the real data. Figure 11 indicates that the frequency-noise models have somewhat larger high-frequency components than the actual data. Even with the excess of high-frequency components, frequency-noise model 1 is remarkably similar to the actual data.

The second set of fits, figures 13–15, covers a shorter time interval. Again, the phase-noise models seem to have a deficit of low-frequency components, while the slowing-down-noise models seem to lack the high frequencies needed to produce the abrupt changes in slope which are present in the real data. The frequency-noise models, although slightly deficient in high-frequency components, most closely resemble the real data.

The abrupt changes of slope led the Lick group to suggest the occurrence of miniglitches (Nelson *et al.* 1970). In the frequency-noise models, the changes in slope are caused not by a single event, but by a statistical fluctuation in the number of events in the neighborhood of a slope change. The individual frequency jump of 2.3×10^{-9} Hz is too small to be seen in any of the figures; in our pseudo-data they occur at a rate of about four per day. If one assumes that there were only four frequency jumps in the period 1969 December through 1970 May, as in Nelson *et al.* (1970), then one must assume that the observed changes in n are indications of changes in the radiation mechanism. It is hard to see how this could come about, given the observed constancy of the pulse shape. On the other hand, the interpretation presented here allows an intrinsically constant braking index: the observed changes caused by the perturbations arising from the noise (cf. eq. [19]).

Another interesting feature of the pseudo-data residuals, appearing in figures 14 and 15, is their resemblance to the quasi-sinusoidal structure reported by Arecibo (see fig. 4).

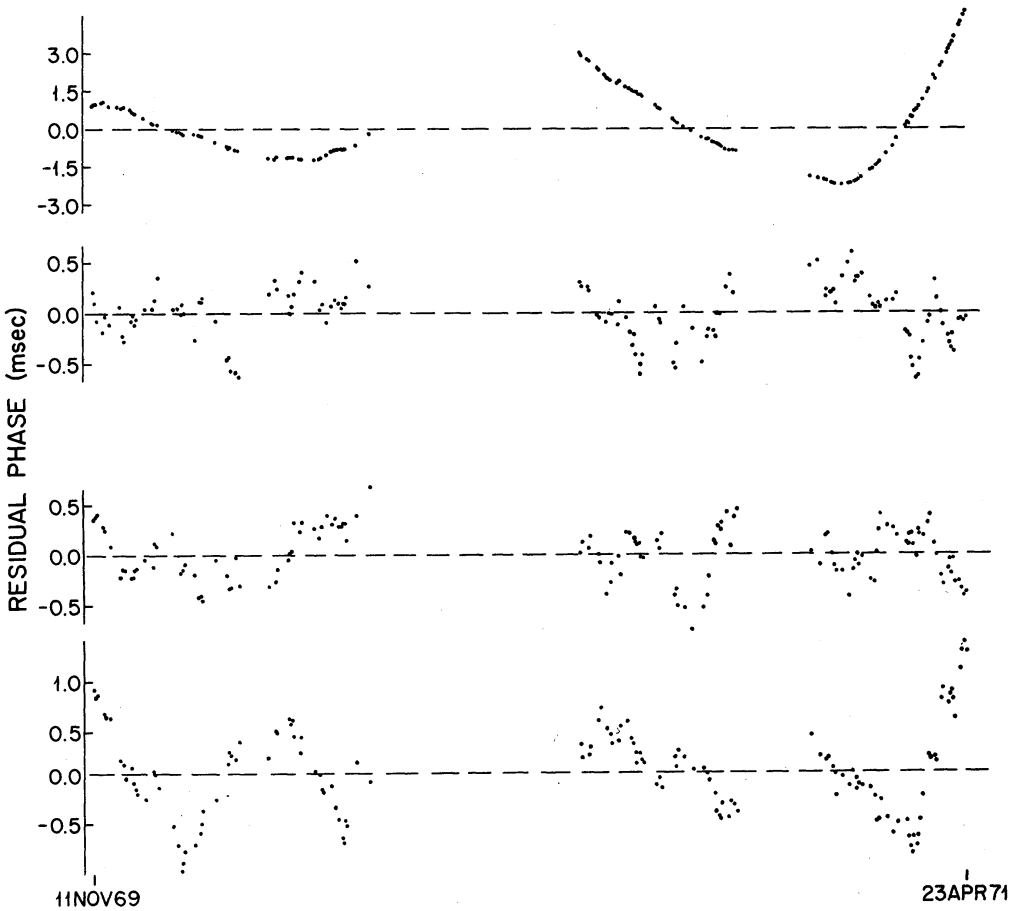

FIG. 10.—Residuals from cubic fits to phase noise pseudo-data. *Top*, real data, 1969 November 11–1971 April 23. Next in order: phase-noise pseudo-data Nos. 1, 2, and 3.

Again, it should be emphasized that this structure results solely from the random superposition of small, discrete events. There is no need to introduce a wobble (Ruderman 1970*b*), an orbiting companion (Richards *et al.* 1970; Hills 1970), or vortex line oscillations (Ruderman 1970*a*).

From the discussion given above, we conclude that the frequency-noise models resemble most closely the actual data, and a comparison of the amplitudes gives 2×10^{-22} $\mathrm{Hz}^2\ \mathrm{s}^{-1}$ as a third estimate of $R\langle\Delta\nu^2\rangle$. The phase-noise and slowing-down-noise models seem to be rougher and smoother, respectively, than the real data. It may be that all three processes are occurring simultaneously. In this case, the low-frequency region of the power spectrum would be dominated by slowing-down noise, the intermediate-frequency region by frequency noise, and the high-frequency region by phase noise.

VI. PHYSICAL MODELS FOR THE NOISE COMPONENT

Two simple mechanisms for producing frequency-jump noise in NP 0532 are presented here. There are other possible mechanisms, but the point is that plausible processes can easily produce the proposed noise component in the timing data. In fact, one would be surprised if one or both of those processes were not operating on the pulsar.

The first model to be considered is an accretion model (Groth 1971). One imagines that lumps of matter fall on the pulsar, causing it to speed up or slow down, mainly through the mechanism of angular-momentum transfer. The mass of the lump can be related to the size of the frequency increment; and the measured quantity, $R\langle\Delta\nu^2\rangle$ (eq. [28]), pro-

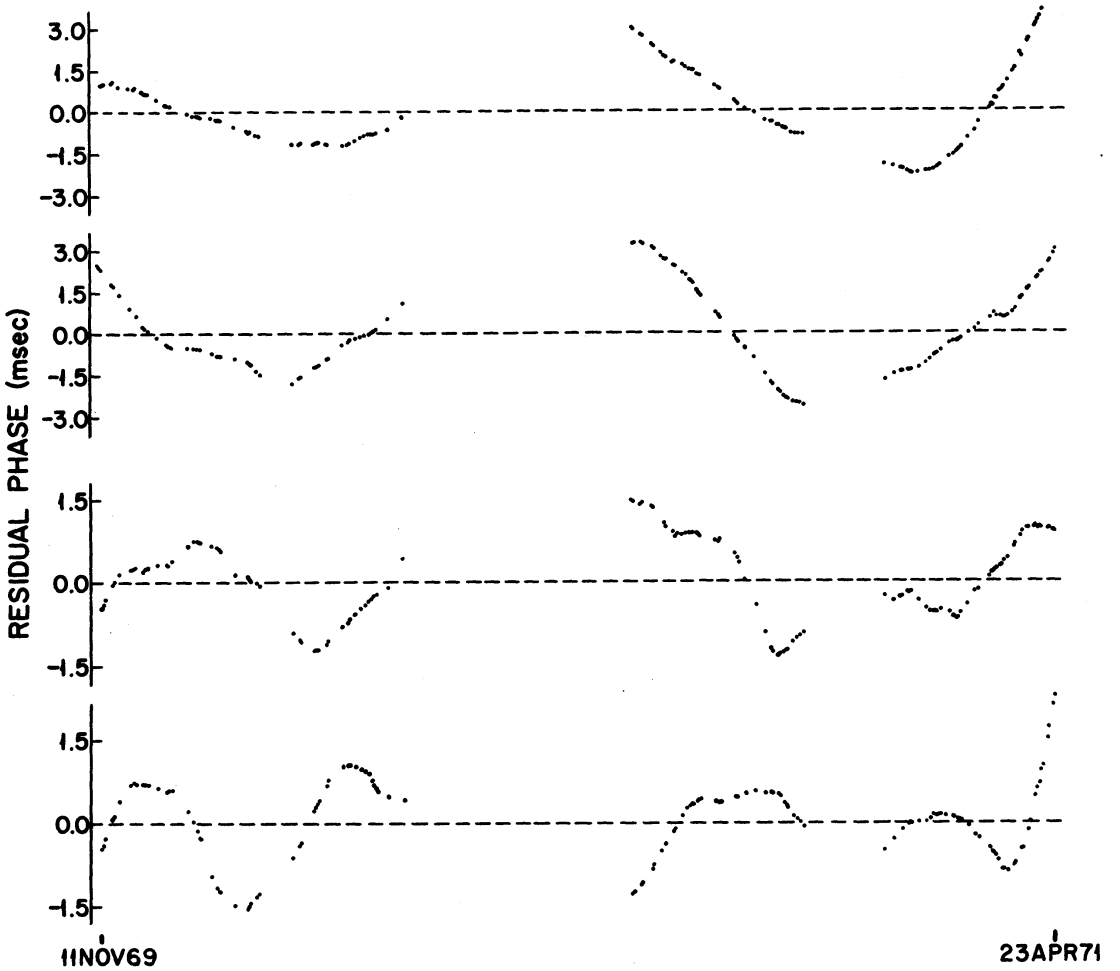

FIG. 11.—Residuals from cubic fits to frequency-noise pseudo-data. *Top*, real data, 1969 November 11–1971 April 23. Next in order: frequency-noise pseudo-data Nos. 1, 2, and 3.

vides a means of relating the rate of mass accretion to the average frequency jump. Suppose a lump of mass m starts from rest very far away and falls onto the pulsar. The maximun change in angular momentum will be

$$\Delta L = m(2GMr_p)^{1/2} . \tag{32}$$

In this expression, L is the angular momentum of the pulsar, $M \approx 1\ M_\odot$ is the pulsar mass, $r_p \approx 10$ km is its radius, and G is the gravitational constant. The change in frequency can be related to the change in angular momentum and hence to the mass of the lump by

$$\frac{m}{M} \approx 3\Delta\nu\left[\frac{8\pi^2}{25}\left(\frac{r_p}{r_0}\right)\left(\frac{r_p^2}{c^2}\right)\right]^{1/2} . \tag{33}$$

The factor of three has been included because only the component of ΔL parallel to L leads to a change in frequency. Also, the gravitational radius of the pulsar has been denoted by r_0. Numerically, equation (33) becomes

$$m/M_\odot \approx 1.5 \times 10^{-2}(\Delta\nu/\nu) . \tag{34}$$

If we assume $\Delta\nu_{\rm rms} \approx \langle\Delta\nu^2\rangle^{1/2}$ and adopt $R\langle\Delta\nu^2\rangle \approx 10^{-22}$ Hz^2 s^{-1}, then we find

$$dM/dt \approx 10^{-19}(\Delta\nu/\nu)^{-1}\, M_\odot \text{ year}^{-1} . \tag{35}$$

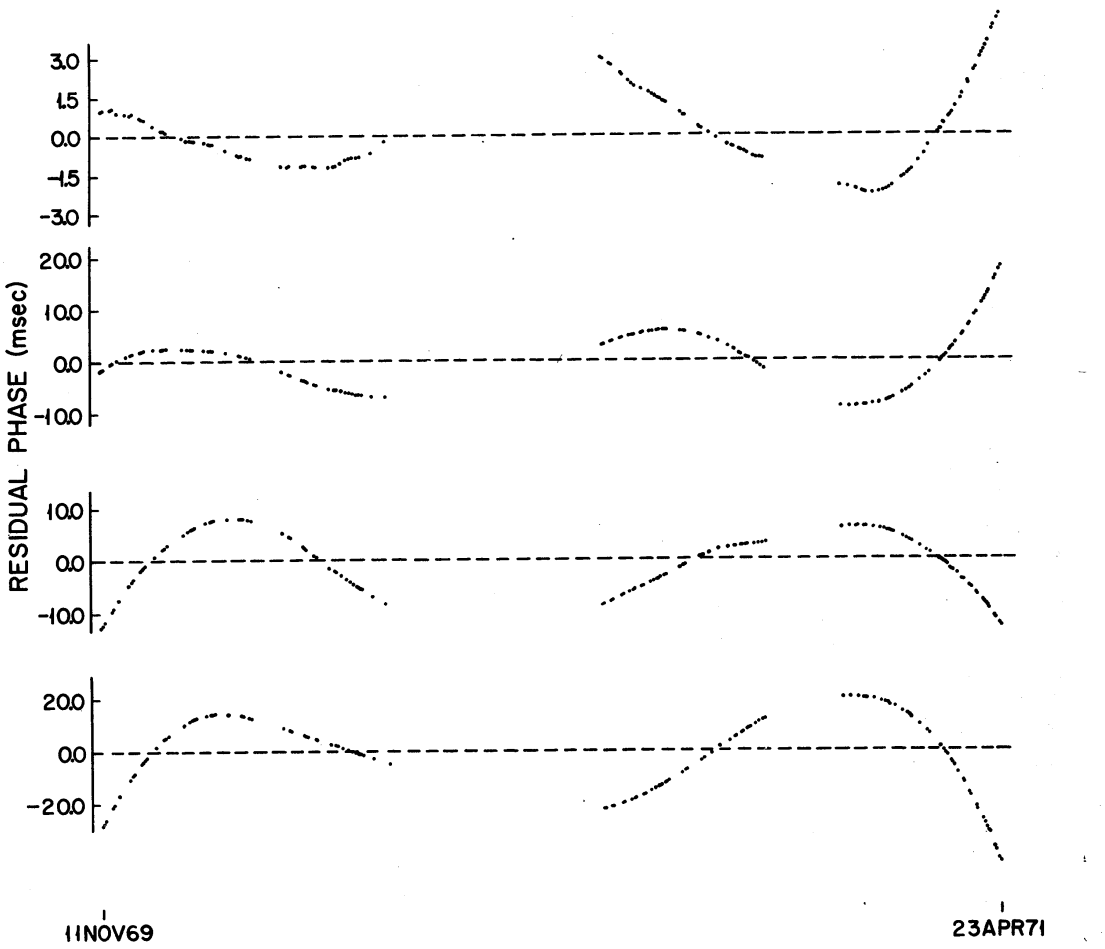

FIG. 12.—Residuals from cubic fits to slowing-down-noise pseudo-data. *Top*, real data, 1969 November 11–1971 April 23. Next in order: slowing-down-noise pseudo-data Nos. 1, 2, and 3.

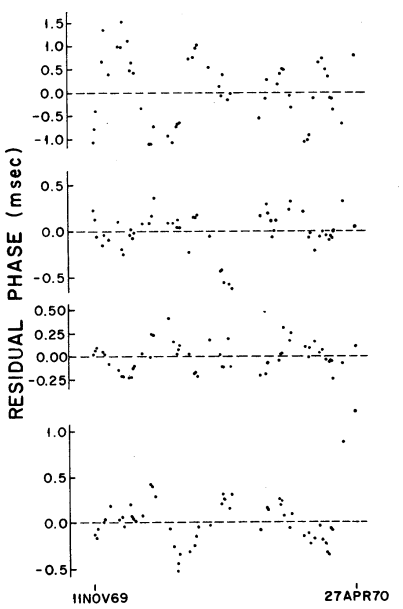

FIG. 13

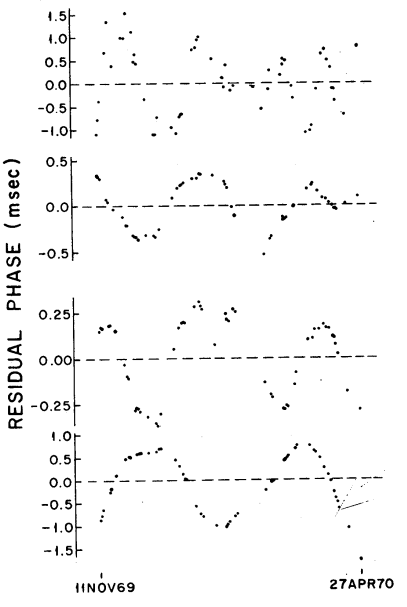

FIG. 14

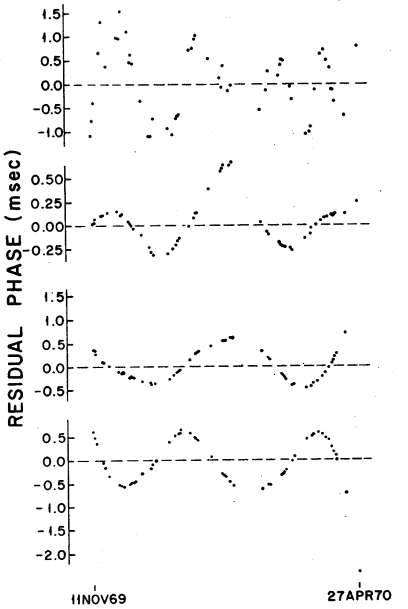

FIG. 15

FIG. 13.—Residuals from cubic fits to phase-noise pseudo-data. *Top*, real data, 1969 November 11–1970 April 27. Next in order: phase-noise pseudo-data Nos. 1, 2, and 3.

FIG. 14.—Residuals from cubic fits to frequency-noise pseudo-data. *Top*, real data, 1969 November 11–1970 April 27. Next in order: frequency-noise pseudo-data Nos. 1, 2, and 3.

FIG. 15.—Residuals from cubic fits to slowing-down-noise pseudo-data. *Top*, real data, 1969 November 11–1970 April 27. Next in order: slowing-down-noise pseudo-data Nos. 1, 2, and 3.

Relations (34) and (35) are shown in figure 16. It can be seen that there is a large range of $\Delta\nu/\nu$ which require quite reasonable lump masses and mass-accretion rates. For example, at $\Delta\nu/\nu = 10^{-10}$, the lump size is $10^{-12}\ M_\odot$, about the mass of a medium-sized asteroid, and the accretion rate is $10^{-9}\ M_\odot$ year^{-1}, which is quite negligible even if mass has been accreting at this rate since the pulsar was born. At this value of $\Delta\nu/\nu$, a lump falls on the pulsar about once a day on the average.

Another model is the cracking model, similar to the continuous crumbling model proposed by Papaliolios *et al.* (1970). In the present context, however, the model is used to introduce randomness, rather than to explain the fact that the braking index is not 3. The pulsar is assumed to be a solid, slightly oblate spheroid. The moment of inertia is given by

$$I = I_0(1 + 2\epsilon)\,, \tag{36}$$

where I_0 is $\frac{2}{5}Mr_p^2$ and ϵ is the ellipticity. The star is assumed to crack slightly, causing a change in the ellipticity which can be related to the change in the pulse frequency,

$$\Delta\epsilon = -\frac{1}{2}\frac{\Delta\nu}{\nu}\,. \tag{37}$$

A reasonable distribution for the amplitudes of the cracks would be

$$p(\Delta\epsilon) = \frac{1}{\Delta\epsilon_0}\exp\left(-\Delta\epsilon/\Delta\epsilon_0\right)\,, \tag{38}$$

where $p(\Delta\epsilon)$ is the probability density at $\Delta\epsilon$. In this case, $\langle\Delta\epsilon\rangle = \Delta\epsilon_0$ and $\langle\Delta\epsilon^2\rangle = 2(\Delta\epsilon_0)^2$. The rate of change in ellipticity due to cracking can be related to the average change in pulse frequency,

$$\left.\frac{d\epsilon}{dt}\right|_{\text{CRACKING}} = -5\times 10^{-26}\left(\frac{\Delta\nu}{\nu}\right)^{-1}\,. \tag{39}$$

Relations (37) and (39) are shown in figure 16.

Because NP 0532 is slowing down, the equilibrium ellipticity is decreasing at the rate

$$\left.\frac{d\epsilon}{dt}\right|_{\text{EQUILIBRIUM}} = 2\epsilon\frac{\ddot{\nu}}{\nu} = -3\times 10^{-15}\ \text{s}^{-1}\,. \tag{40}$$

Assuming that cracking keeps the ellipticity in equilibrium, equations (39) and (40) can be combined to yield an estimate for $\Delta\nu/\nu$:

$$\Delta\nu/\nu = 1.6\times 10^{-11}\,. \tag{41}$$

Using $R = 2\times 10^{-22}$ Hz^2 s$^{-1}/2(\Delta\nu)^2$ (the factor of 2 enters because $\langle\Delta\nu\rangle^2 = \frac{1}{2}\langle\Delta\nu^2\rangle$), we find that the average rate is about 40 cracks per day. Again, these parameters are quite reasonable, and it appears that the cracking model is also a plausible means of explaining the structure in the data.

In connection with figure 16 it should be noted that an event rate as small as once per month is only marginally consistent with the observed structure in the data. There sometimes appears to be significant structure on a timescale as short as a week. Adopting a lower limit of one per week for R implies an upper limit of about 2×10^{-10} for $\Delta\nu/\nu$. This upper limit is about two orders of magnitude smaller than the size of the glitch and indicates that the glitch is probably not part of the noise component.

VII. CONCLUSIONS

It has been shown that the pulse frequency of NP 0532 in the 2-year period 1969 March–1971 April can be understood in terms of three components. The major compo-

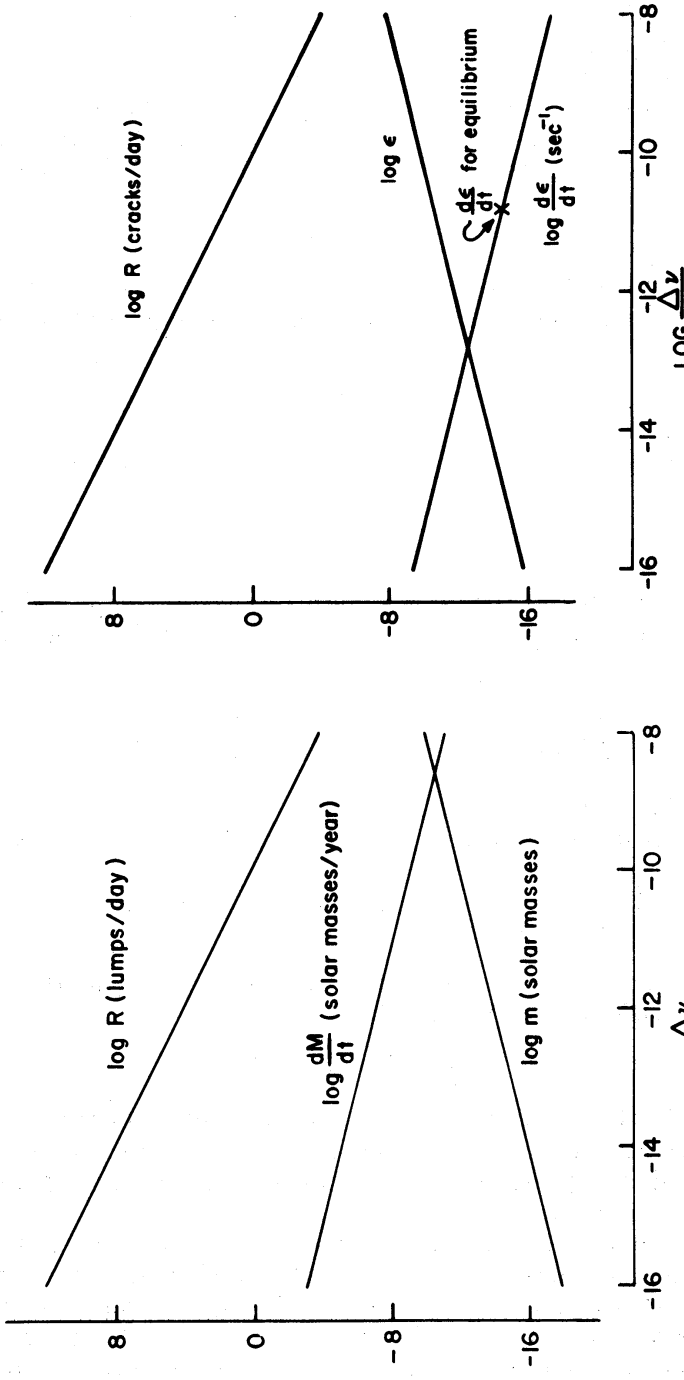

FIG. 16.—Physical noise model parameters as a function of $\Delta\nu/\nu$. *Left*, accretion model; *right*, cracking model.

nent is the cubic braking function. Unfortunately, the braking index of 2.4 given in equation (5) does not point to any simple braking mechanism. However, the data are consistent with a time-independent braking mechanism.

The second component is the frequency jump which occurred on 1969 September 29. This glitch can best be understood in terms of a two-component model of neutron-star structure. The glitch parameters given in equations (7)–(10) are consistent with this model.

Finally, there is a noise component which can be understood in terms of small random jumps in the pulsar frequency. The dispersion in ν as a function of the length of data used to estimate ν is probably the strongest indication that frequency noise is the predominant noise component. More progress will be made with the power spectrum and Monte Carlo techniques as the data string increases in length allowing the power spectrum to be extended to lower frequencies.

We wish to acknowledge the assistance of J. D. Mulholland for providing the JPL ephemeris and D. W. Richards who provided the Arecibo arrival times. The members of the Princeton University Observatory and the Princeton University Computer Center were most cooperative. Discussions with J. N. Bahcall, V. M. Bearg, K. C. Davis, R. H. Dicke, P. S. Henry, M. R. Nelson, P. J. E. Peebles, D. Pines, and R. Ruffini were extremely helpful. One of us (E. J. G.) is grateful for the support of an NSF graduate fellowship.

REFERENCES

Baym, G., Pethick, C., Pines, D., and Ruderman, M. 1969, *Nature*, **224**, 872.
Baym, G., and Pines, D. 1971, *Ann. Phys.*, **66**, 816.
Boynton, P. E., Groth, E. J., Partridge, R. B., and Wilkinson, D. T. 1969*a*, *Ap. J.* (*Letters*), **157**, L197.
———. 1969*b*, *IAU Circ.*, No. 2179.
Ferrari, A., and Ruffini, R. 1969, *Ap. J.* (*Letters*), **158**, L71.
Greenstein, G. S., and Cameron, A. G. W. 1969, *Nature*, **222**, 862.
Groth, E. J. 1971, Ph.D. thesis, Princeton University.
Gunn, J. E., and Ostriker, J. P. 1969, *Nature*, **221**, 454.
Hills, J. G. 1970, *Nature*, **226**, 730.
Hoffman, B. 1968, *Nature*, **218**, 667.
Horowitz, P., Papaliolios, C., Carleton, N. P., Nelson, J., Middleditch, J., Hills, R., Cudaback, D., Wampler, J., Boynton, P. E., Groth, E. J., Partridge, R. B., Wilkinson, D. T., Duthie, J. G., and Murdin, P. 1971, *Ap. J.* (*Letters*), **166**, L91.
Michel, F. C. 1970, *Ap. J.* (*Letters*), **159**, L25.
Michel, F. C., and Tucker, W. H., 1969, *Nature*, **223**, 277.
Minkowski, R. 1966, in *Stars and Stellar Systems*, Vol. **8**, *Stellar Structure*, ed. L. H. Aller and D. B. McLaughlin (Chicago: University of Chicago Press), p. 639.
Nelson, J., Hills, R., Cudaback, D., and Wampler, J. 1970, *Ap. J.* (*Letters*), **161**, L235.
O'Handley, D. A., Holdridge, D. B., and Mulholland, J. D. 1969, JPL External Tech. Rept.
Ostriker, J. P., and Gunn, J. E. 1969, *Ap. J.*, **157**, 1395.
Pacini, F. 1967, *Nature*, **216**, 567.
Papaliolios, C., Carleton, N. P., and Horowitz, P. 1970, *Nature*, **228**, 445.
Radhakrishnan, V., and Manchester, R. A. 1969, *Nature*, **222**, 228.
Rankin, J. M., and Roberts, J. A. 1970, *IAU Symposium No. 46, The Crab Nebula*, Jodrell Bank, Great Britain.
Reichley, P. E., and Downs, G. E. 1969, *Nature*, **222**, 229.
Rice, S. O. 1954, in *Noise and Stochastic Processes* (New York: Dover Publications), p. 162.
Richards, D. W., Pettengill, G. H., Counselman, C. C., III, and Rankin, J. M. 1970, *Ap. J.* (*Letters*), **160**, L1.
Richards, D. W., Pettengill, G. H., Roberts, J. A., Counselman, C. C., III, and Rankin, J. M. 1969, *IAU Circ.*, No. 2181.
Ruderman, M. 1969, *Nature*, **223**, 597.
———. 1970*a*, *ibid.*, **225**, 619.
———. 1970*b*, *ibid.*, p. 838.
Shapiro, I. I. 1964, *Phys. Rev. Letters*, **13**, 789.
Trimble, V. 1968, *A.J.*, **73**, 535.